



An Insight into the Hormonal Interplay Regulating Pigment Changes and Colour Development in the Peel of ‘Granny Smith’, ‘OPAL[®]’ and ‘Royal Gala’ Apples

Pablo Fernández-Cancelo¹ · Jordi Giné-Bordonaba¹ · Neus Teixidó¹ · M. Carmen Alamar²

Received: 3 August 2023 / Accepted: 17 February 2024
© The Author(s) 2024

Abstract

Three apple cultivars with different peel colour and known ripening dynamics were examined throughout development and on-tree ripening to unravel how the hormonal crosstalk may influence colour changes. Our results indicate that the colour of ripe apples in ‘Granny Smith’ and ‘Opal[®]’ cultivars was primarily influenced by chlorophyll levels masking the contribution of other pigments, whilst the development of red colour in the ‘Royal Gala’ was not only due to an important loss of chlorophyll during ripening but also to anthocyanins accumulation. The interplay amongst indole-3-acetic acid (IAA), ethylene and abscisic acid (ABA) seemed to control pigment content during the later stages of development, indicating that variations in the hormonal profile contribute to colour differences in ripe apples. In ‘Granny Smith’ apples, basal levels of IAA, ethylene and ABA were associated with the inhibition of chlorophyll loss, which was responsible for its green colour, despite the presence of high carotenoid levels. In contrast, the peel of ‘Opal[®]’ and ‘Royal Gala’ apples underwent a degreening process facilitated by the IAA-mediated activation of ethylene metabolism, in a crosstalk facilitated by *MdARF5*. The accumulation of anthocyanins in the peel of ‘Royal Gala’ apples seemed to be regulated in an ethylene-dependent manner, with *MdMYB1* acting as the mediator between ethylene signalling and the anthocyanins biosynthesis and vacuolar transport pathways. On the other hand, the decline in carotenoid content during fruit development in the three cultivars appeared to be regulated at the catabolic level through ABA and its derivatives and possibly also facilitated by ethylene-mediated mechanisms. Notably, chlorophyll levels, crucial for the observed colour changes, were likely controlled by *MdGLK1*, a transcription factor involved in chloroplast biogenesis, working in coordination with ethylene-dependent catabolic enzymes. Overall, understanding the cultivar-specific hormonal regulation of apple colour provides valuable insights for developing preharvest and postharvest strategies to ensure an optimal fruit colour aligned with consumer preferences.

Keywords Abscisic acid · Anthocyanins · Carotenoids · Chlorophylls · Ethylene · *MdARF5* · *MdGLK1*

Introduction

Fruit colour significantly impacts consumer perception and acceptance, not only because it serves as an indicator of ripeness and quality, but also because of its impact with human

health benefits (Dar et al. 2019). For instance, carotenoids play a crucial role in maintaining healthy vision due to their involvement in retinol biosynthesis whilst anthocyanins are potent antioxidants which reduce the risk of multiple chronic diseases (De Pascual-Teresa and Sanchez-Ballesta 2008; Eggersdorfer and Wyss 2018).

Colour development in fruit is linked to the balance amongst pigments, which in turn is modulated by signalling pathways involving a complex interplay amongst hormones, transcription factors and response to environmental stimuli (Liu et al. 2021). Generally, during the first stages of fruit development, cytokinins, and the transcription factor GOLDEN2-LIKE (GLK) are key hormones and signalling components, respectively, participating in chloroplast biogenesis and the accumulation of chlorophylls, the pigments

Handling Author: Raul Herrera.

✉ M. Carmen Alamar
m.d.alamargavidia@cranfield.ac.uk

¹ Postharvest Programme, Institute of Agrifood Research and Technology (IRTA), Edifici Fruitcentre, Parc Agrobiotech Lleida, Parc de Gardeny, 25003 Lleida, Spain

² Plant Science Laboratory, Cranfield University, Cranfield MK43 0AL, UK

responsible for the green colour of unripe fruit (An 2019; Cackett et al. 2022; Cortleven and Schmölling 2015). As fruit mature, chlorophyll levels tend to decrease allowing the emergence of other pigments, such as carotenoids and anthocyanins, responsible for the characteristic yellow and red colour in ripe fruit, respectively (Reay et al. 1998).

In climacteric fruit, ethylene predominantly stimulates chlorophyll degradation by inducing genes encoding chlorophyll catabolic enzymes, including NON-YELLOW COLOURING1 (NYC1), NYC1-LIKE (NOL), PHEOPHYTINASE (PPH), and PHEOPHORBIDE A OXIGENASE (PAO) (Wei et al. 2021). However, ethylene not only contributes to chlorophyll degradation but also promotes expression of MYB1, a transcription factor that enhances the expression of anthocyanins biosynthetic genes, such as the *DIHYDROFLAVONOL 4-REDUCTASE (DFR)*, *ANTHOCYANIDIN SYNTHASE (ANS)*, and *UDP-GLUCOSE:FLAVONOID 3-O-GLUCOSYLTRANSFERASE (UFGT)*, which in turn favour the development of red colour in apples (Liu et al. 2021). Carotenoids, on the other hand, contribute to the yellow colour in apples and serve as precursors for the biosynthesis of abscisic acid (ABA), a hormone that orchestrates various aspects of fruit development and ripening in non-climacteric fruit and occasionally, in coordination with ethylene, also in climacteric fruit including apples (Fernández-Cancelo et al. 2022b; Gupta et al. 2022; Mou et al. 2016). Whilst carotenoids accumulate during fruit development in tomatoes, a model fruit for climacteric ripening, they tend to dwindle during apple development and ripening (Fernández-Cancelo et al. 2022a; Llorente et al. 2016). Hence, the surge of yellow colour, in certain apple varieties, results from the depletion of chlorophylls rather than carotenoids accumulation (Fernández-Cancelo et al. 2022a; Knee 1972). It is well documented that both in tomatoes and apples, the rate-limiting step of carotenoids biosynthesis is regulated by *PHYTOENE SYNTHASE (PSY)* (Ampomah-Dwamena et al. 2022, 2015; Zhou et al. 2022). The expression of *PSY* is negatively regulated by *PHYTOCHROME-INTERACTING FACTORS (PIF)*, a family of transcription factors involved in environmental stimuli and hormonal signalling integration in Arabidopsis and tomato (Cruz et al. 2018; Lucas and Prat 2014).

Although ethylene is considered the key regulator of colour development during climacteric fruit ripening, recent studies suggested that other hormones, such as IAA and ABA, may participate, either alone or in cooperation with ethylene, in triggering ripening-related changes in climacteric fruit, including tomatoes, pears, peaches and apples (Chaabouni et al. 2009; Fernández-Cancelo et al. 2022b; García-Pastor et al. 2021; Lindo-García et al. 2020; Tatsuki et al. 2013).

Despite increasing research on the IAA-ethylene-ABA crosstalk regulating fruit biochemical changes during

development, the role of these hormones in regulating colour changes in apples, and in other fruit, remains elusive. Accordingly, our study aims to investigate, both at biochemical and gene expression level, the potential influence of the interplay amongst ethylene, IAA, ABA and cytokinins in the pigment levels and colour changes during the development and ripening of different apple cultivars distinguished by their peel colour.

Material and Methods

Plant Material and Experimental Design

In 2021, three apple cultivars—‘Granny Smith’, ‘Opal[®]’ and ‘Royal Gala’—were chosen to investigate their colour changes during development and on-tree ripening. These cultivars were selected based on their commercial relevance in the Ebro Valley (Spain), ethylene production capacity and/or their distinct peel colour. Specifically, ‘Granny Smith’ apples present green colour even when they are ripe, whereas ‘Opal[®]’ and ‘Royal Gala’ show yellow and red colour, respectively, in the final fruit developmental stages.

The studied apple cultivars were sampled from the same commercial orchard located in Alcarràs, Lleida, Spain. These cultivars exhibited similar blooming times, with a maximum difference of five days amongst them. ‘Opal[®]’ apples started their blooming period five days earlier than the ‘Royal Gala’ and ‘Granny Smith’ cultivars, which shared identical blooming times.

The first four sampling points were performed simultaneously for all three cultivars every 25–30 days. The fourth sampling point (S4) coincided with the commercial harvest date (CHD) of the ‘Royal Gala’ apples, which occurred 125 days after full bloom (DAFB) for ‘Royal Gala’ and ‘Granny Smith’ and 130 DAFB for ‘Opal[®]’. However, since ‘Granny Smith’ and ‘Opal[®]’ apples required additional time to achieve commercial maturity, two extra sampling points were included for these cultivars. The fifth sampling point (S5) corresponded to 151 DAFB for ‘Granny Smith’ and 156 DAFB for ‘Opal[®]’, whilst the sixth sampling point (S6) and CHD were established at 173 DAFB for ‘Opal[®]’ and 172 DAFB for ‘Granny Smith’ (Fig. 1A).

To conduct our analysis, 20 trees were randomly selected for each cultivar and apples were collected from the mid-outer canopy at the same height, as well as from both sides of the tree that were exposed and non-exposed to the sun. For each cultivar and sampling point, 20 fruit were used for colour instrumental evaluations. Additionally, for each cultivar and sampling point, 40 apples (10 apples per replicate and four replicates) were peeled and the peel from the coloured face snap-frozen in liquid nitrogen, ground and stored

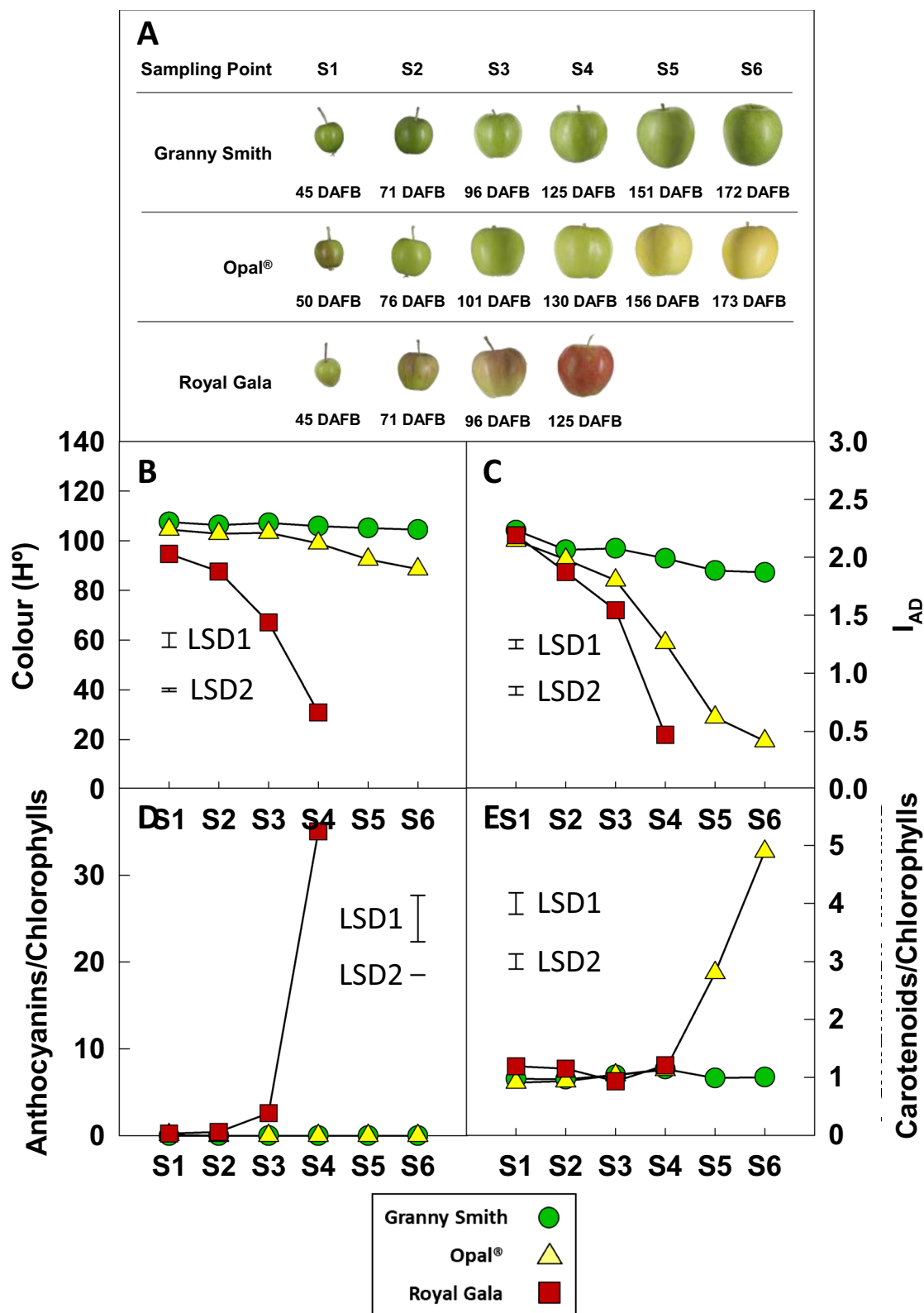


Fig. 1 Peel colour changes (A), Hue angle (B), I_{AD} (C), ratio anthocyanins/chlorophylls and ratio carotenoids/chlorophylls (D) during the development and ripening of ‘Granny Smith’ (●), ‘Opal®’ (▲) and ‘Royal Gala’ (■) apples. Each point represents the mean of four bio-

logical replicates (10 apples per replicate). Error bars represent the LSD values ($p=0.05$) for the interaction cultivar×sampling point for all cultivars from S1 to S4 (LSD1) and for the interaction cultivar×sampling point for ‘Opal®’ and ‘Granny Smith’ from S1 to S6 (LSD2)

at -80°C until further biochemical analysis. A portion of the frozen and ground sample was freeze-dried for 72 h to conduct the biochemical analysis of hormones, pigments and phenolic compounds.

Determination of Colour Parameters

Within a time frame of less than two hours after harvest, colour and the Index of Absorbance Difference (I_{AD}) were measured on the coloured face of 20 individual fruit per cultivar and sampling point. The objective evaluation of colour was performed using a portable colorimeter (CM-2600d; Konica Minolta Sensing, Osaka, Japan) to determine the Hue angle, a colorimetric parameter representing the type of colour perceived on a 360° scale, where 0° represents maximum redness, 90° maximum yellowness and 180° maximum greenness (Scalisi et al. 2022).

A DA-meter (FR Turoni, Forlì, Italy) was used to measure the I_{AD} index. The I_{AD} index is commonly used to evaluate the ripening stage of the fruit by measuring the difference in absorbance between chlorophyll *a* (670 nm) and the background spectrum (720 nm). The I_{AD} index ranges from 0.0 to 2.2, where a value 2.2 represents high chlorophyll content and 0.0 represents absence of chlorophyll (Zhang et al. 2017).

Hormonal Profiling

Endogenous phytohormones were extracted by mixing 100 mg of the freeze-dried apple peel samples with 5 mL methanol:water:formic acid, 60:35:5 (v/v/v) and 50 μL of Deuterium-labelled internal standards (100 ng mL^{-1}). The mixture was vortexed for 2 min at 2000 rpm, kept in ice and dark for 20 min and centrifuged at 4500 g for 10 min at 4°C . The supernatant was recovered and freeze-dried overnight. The freeze-dried samples were dissolved with 0.5 mL methanol:water:formic acid 1:9:0.1 solution (v/v/v) containing ammonium formate (1 mM), vortexed at 2000 rpm for 3 min and centrifuged at 4500 g for 10 min at 4°C . The supernatant was collected and filtered through 0.22- μm PTFE filter into silanized amber vials. Hormones separation and identification were carried out according to Collings et al. (2023). Briefly, 10 μL of extract were injected on a LC-MS/MS instrument with an Agilent 1200 series HPLC system (Agilent, Berkshire, United Kingdom) coupled with a Q-Trap 6500 mass spectrometer (AB Sciex, Framingham, MA, USA), and equipped with a Hypersil GOLD C18 column ($50 \times 2.1\text{ mm}$, $1.9\text{ }\mu\text{m}$; Thermo Fisher Scientific, Waltham, MA, USA) held at 30°C . Separation was carried out at a flow rate of 0.4 mL min^{-1} using a mobile phase consisting in a mixture of 0.1% formic acid and ammonium formate (1 mM) in water (A) and 0.1% formic acid and ammonium formate (1 mM) in methanol (B), using an

increasing gradient of B (5% for 1 min, 40% at 5 min, 95% at 6.5 min which was hold for 1 min, then back to 5% at 8.5). The concentration of the plant hormones was quantified using a 10-point calibration curve ranging from 1 ng mL^{-1} to 250 ng mL^{-1} for each analysed phytohormone, and it was expressed in $\mu\text{g kg}^{-1}$ dry weight (DW). Deuterated and non-deuterated ABA metabolites: (+)-ABA-glucose ester (ABA-GE), (–)-phasic acid (PA), (–)-dihydrophasic acid (DPA), (–)-neo-PA (neo-PA), and (\pm)-7'-OH-hydroxy-ABA (7-OH-ABA) were purchased from the National Research Council of Canada—Plant Biotechnology Institute (Saskatoon, SK, Canada); (\pm)-ABA was obtained from Sigma-Aldrich (Darmstadt, Germany); and the deuterated and non-deuterated indole-3-acetic acid (IAA), isopentenyladenine (iP), isopentenyladenosine (iPR) *trans*-zeatin (*tZ*), *cis*-zeatin (*cZ*), *trans*-zeatin (*tZR*), *cis*-zeatin riboside (*cZR*), dihydrozeatin (DZ) and dihydrozeatin riboside (DZR) were purchased from OlChemIm, Olomouc, Czech Republic. The content of active cytokinins was calculated by summing the concentrations of iP, *tZ*, *cZ* and DZ.

Phenolic Compounds and Anthocyanins Identification and Quantification

Phenolic compounds were extracted following the protocol described by (Fernández-Cancelo et al. 2022a), with some modifications. Briefly, 50 mg of freeze-dried peel tissue were mixed with 1 mL of 79.5% (v/v) methanol and 0.5% (v/v) HCl in Milli-Q water, incubated in a water bath for 30 min at 35°C and centrifuged at 20,000 g for 30 min at room temperature. The extract was filtered through 0.22- μm PTFE filter and injected (10 μL) on an Agilent 1200 liquid chromatograph (Agilent Technologies, Santa Clara, CA, USA) fitted with an Eclipse XDB-C18 column ($250 \times 4.6\text{ mm}$, $5.0\text{ }\mu\text{m}$; Agilent Technologies, Santa Clara, CA, USA). Based on Anastasiadi et al. (2017), phenolic compounds separation was performed at flow rate of 1 mL min^{-1} with mobile phases consisting of 0.1% formic acid in water (A) and acetonitrile (B). The gradient increased linearly from 0% B to 15% B in 15 min, then raised to 22% B in 21 min and finally elevated to 100% B in 5 min and held at 100% B for 5 min. The separation of procyanidin B2 and anthocyanins was performed in a Kinetex LUNA C18 column ($250 \times 4.6\text{ mm}$, $5.0\text{ }\mu\text{m}$; Phenomenex Inc., Torrance; CA, USA) with mobile phases consisting of 0.1% formic acid in water (A) and methanol (B). The flow rate was 1 mL min^{-1} and the gradient used increased linearly from 0% B to 20% B in 20 min, then raised to 28% B in 10 min followed by an increase to 38% in 25 min and finally elevated to 100% B in 3 min and held at 100% B for 5 min. In both separations, column temperature was kept at 35°C and the sample compartment was refrigerated at 10°C . Detection was performed at 280, 320, 360, and 520 nm, yet the online spectra

were acquired in the 220–650-nm wavelength range with a resolution of 0.5 nm. Phenolic compounds were identified according to their retention time, spectral features and ratios of maximum absorption peaks (λ). Quantification was performed using calibration curves prepared with standard stock solutions of cyanidin 3-O-galactoside, procyanidin B1, procyanidin B2, chlorogenic acid, catechin, epicatechin, quercetin-3-O-rutinoside and phloretin-2'-O-glucoside and their concentrations were expressed as g kg^{-1} DW. When no commercial standard was available, detected cyanidin, quercetin and phloretin derivatives were quantified using cyanidin 3-O-galactoside, quercetin-3-O-rutinoside and phloretin-2'-O-glucoside standard curves, respectively.

Carotenoids and Chlorophylls Analysis

Carotenoids and chlorophylls were extracted based on the method described by Alagoz et al. (2020) by mixing 100 mg of freeze-dried peel tissue with 800 μL of acetone-ethyl acetate (6:4, v/v) solution containing 0.1% butylated hydroxytoluene (BHT) and 0.1% canthaxanthin (0.5 mg mL^{-1}) as internal standard. An equal volume of water was added, samples were mixed by inversion and centrifuged 5 min at 12,000 g at 4 °C. The upper phase was collected and centrifuged again 5 min at 12,000 g and 4 °C. The organic extract was filtered through a 0.22- μm filter and injected (20 μL) on an Agilent 1260 Infinity II liquid chromatograph HPLC fitted with a YMC C30 Carotenoid column (250 mm \times 4 mm i.d., 3 μm ; Teknokroma, Barcelona, Spain) and a guard column of the same material (10 mm \times 4.0 mm, 3 μm). Separation was carried out at a flow rate of 1 mL min^{-1} using a binary gradient elution initially composed by 95% methanol and 5% methyl tert-butyl ether (MTBE), which was increased linearly to 25% MTBE in 15 min, then raised to 40% in 2 min, elevated to 50% in 3 min and finally raised to 100% in 3 min and maintained for 10 min. The temperature of the column was kept at 25 °C and the sample compartment was refrigerated at 10 °C. Detection was performed at 454 nm yet the online spectra was acquired in the 330–700-nm wavelength range with a resolution of 1 nm. Carotenoids and chlorophylls were identified according to their retention time, spectral features, and ratios of maximum absorption peaks (λ). Identified compounds were quantified using an external calibration curve prepared with a canthaxanthin standard stock solution and their canthaxanthin equivalent concentration were expressed as mg kg^{-1} .

RNA Isolation and qPCR Analysis

RNA was extracted from lyophilized peel samples, using the Spectrum™ Plant Total RNA Kit (Sigma-Aldrich, St Louis, MO, United States) following the manufacturer's recommendation. The cDNA synthesis was performed on 1 μg

of RNA (quantified by a NanoDrop 2000 spectrophotometer [Thermo Fisher Scientific, Waltham, MA, USA]) using the SuperScript IV First-Strand Synthesis System (Invitrogen, Carlsbad, CA, United States). The gene expression analysis (Table S1) was performed by mixing KAPA SYBR® Fast qPCR Master Mix (Kapa Biosystems, Inc., Wilmington, MA, United States), 100 nM of each primer, and the corresponding diluted cDNA. The reaction was performed on a 7,500 Real-Time PCR System (Applied Biosystems, Waltham, MA, United States) under the following conditions: 10 s at 95 °C followed by 40 cycles of 95 °C during 15 s and 60 °C for 1 min. A non-template control (NTC) was included using DNA-free water instead of cDNA. A melt curve analysis was performed to check primer specific by including a final amplification cycle at 95 °C for 15 s, 60 °C for 1 min, 95 °C for 30 s and 60 °C for 15 s. Primers used in this study were retrieved from the literature or designed de novo when indicated (Table S1). Relative gene expression was expressed as Mean Normalized Expression (MNE) according to previous studies (Muller et al. 2002) using *Md8283* as a reference gene.

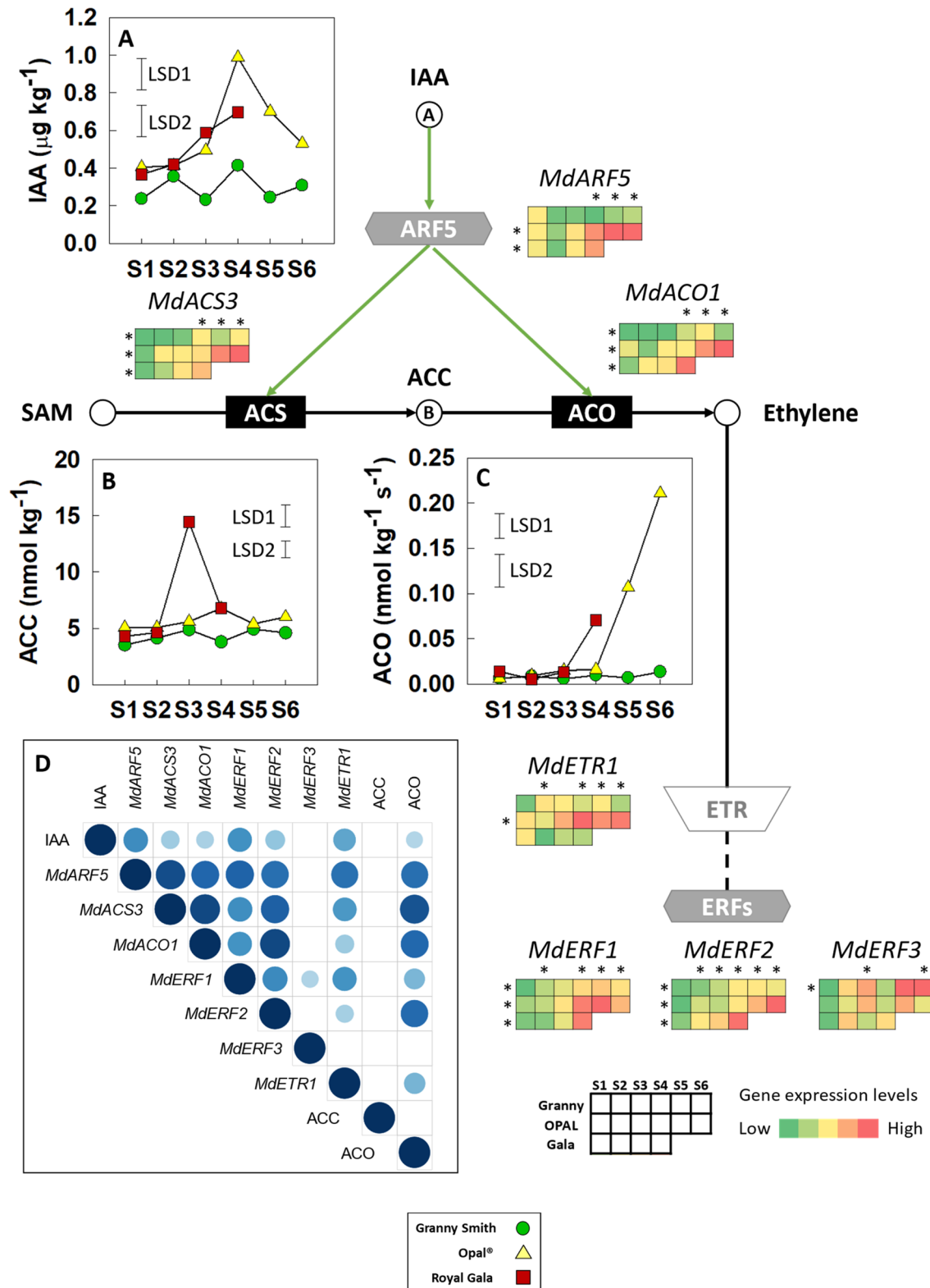
Results

Colour Evolution

'Granny Smith', 'Opal®' and 'Royal Gala' apples differed substantially in their colour evolution during development and on-tree ripening (Fig. 1A). 'Granny Smith' apples maintained their characteristic green colour, with Hue angle values persistently above 105° during development (Fig. 1B). Simultaneously, the I_{AD} for 'Granny Smith' displayed a subtle decline, ranging from 2.2 at S1 to 1.8 at S6 (Fig. 1C). In this apple cultivar, the anthocyanin/chlorophyll and carotenoid/chlorophyll ratios remained low and stable throughout fruit development (Figs. 1D and E).

On the other hand, 'Opal®' apples underwent a noticeable colour shift during development. Beginning with a green colour speckled with red patches at S1, the red colour disappeared in the onward stages and the green colour gradually faded from S2 to S4, before finally adopting a yellow colour at S5 and S6 (Fig. 1A). Accordingly, the Hue angles for 'Opal®' steadily dropped, shifting from 104° at S1 to 88° at S6 (Fig. 1B). Similarly, the I_{AD} followed a declining trend, with a significant decrease from 1.8 at S3 to 0.6 at S5 (Fig. 1C). Whilst the anthocyanin/chlorophyll ratio remained consistently low throughout fruit development, the carotenoid/chlorophyll ratio remained low and steady until it significantly rose at S5 and S6 with values of 2.8 and 4.9, respectively (Figs. 1D and E).

'Royal Gala' apples also changed its colour during development. Starting as a green fruit, red patches gradually



surfaced and spread across its peel after S1. By S4, the red colour covered nearly the entire peel surface (Fig. 1A). The Hue angle significantly dropped from 100° at S1 to 40° at S4, in parallel to the noticeable visual transformation

(Fig. 1B). Likewise, the I_{AD} values also dwindled, initiating at 2.1 at S1 and dropping to 0.5 at S4 (Fig. 1C). In contrast to the other two cultivars, 'Royal Gala' displayed a significant rise in the anthocyanin/chlorophyll ratio during

Fig. 2 Scheme of the crosstalk between indole acetic acid (IAA) and ethylene metabolism showing the evolution of IAA (A), ACC concentration (B) and ACO (ACC OXIDASE activity) (C) and correlations amongst the parameters related with auxin-ethylene hormonal crosstalk (D) during the development and of ‘Granny Smith’ (●), ‘Opal®’ (△) and ‘Royal Gala’ (■) apples. Each point represents the mean of four biological replicates (10 apples per replicate). Error bars represent the LSD values ($p=0.05$) for the interaction cultivar×sampling point for all cultivars from S1 to S4 (LSD1) and for the interaction cultivar×sampling point for ‘Opal®’ and ‘Granny Smith’ from S1 to S6 (LSD2). The corresponding transcript levels of *MdARF5*, *MdACS3*, *MdACO1*, *MdERF1*, *MdERF2*, *MdERF3* and *MdETR1* are represented as heatmaps. Significant differences ($p\leq 0.05$) amongst cultivars at the same sampling point are denoted by asterisks at the top of the heatmaps, whilst differences ($p\leq 0.05$) amongst sampling points at each specific cultivar are indicated by asterisks at the left of the heatmap. Green arrows represent hypothetical positive regulation. Black dashed lines indicate that some steps in the signalling pathway have been omitted. The size of the circle for each correlation and the colour depicts the significance and the correlation coefficient, respectively. Positive correlation coefficients are displayed in blue and negative correlation coefficients in red

fruit maturation, increasing rapidly from 2 at S3 to 35 at S4 (Fig. 1D), whereas the carotenoid/chlorophyll ratios remained low and stable throughout the fruit development (Fig. 1E).

IAA Signalling and Ethylene Metabolism

Throughout their development and on-tree ripening, the apple cultivars ‘Granny Smith’, ‘Opal®’ and ‘Royal Gala’ exhibited distinct variations in the peel content of IAA, *MdARF5* gene expression, and the evolution of the ethylene biosynthetic and signalling pathways (Fig. 2). The levels of IAA and *MdARF5* expression remained steady and below $0.4 \mu\text{g kg}^{-1}$ and 0.04 MNE, respectively, during ‘Granny Smith’ development (Figs. 2A and S1A). In this particular cultivar, the expression of genes associated to ethylene biosynthesis and signalling pathways, as well as the peel 1-aminocyclopropane-1-carboxylic acid (ACC) concentration and ACC OXIDASE (ACO) activity remained low and steady during development and on-tree ripening (Figs. 2B, and C). *MdERF1* gene expression in the peel of ‘Granny Smith’ apples showed a significant increasing trend from 1.7 MNE at S1, culminating at 10.5 MNE at S5 and then decreasing to 8.4 MNE at S6 (Figure S1E). *MdERF3*, in contrast, followed the same trend as in the other cultivars and remained below 0.4 MNE until S5 when increased up to 0.5 MNE and remained in the same level until the time of commercial harvest (Figure S1G).

In contrast, ‘Opal®’ and ‘Royal Gala’ apples exhibited a more dynamic profile regarding IAA and ethylene metabolism and signalling. In both cultivars, IAA levels showed a parallel trend, remaining stable at $0.4 \mu\text{g kg}^{-1}$ from S1 to

S3 and then rising to $0.70 \mu\text{g kg}^{-1}$ and $1.0 \mu\text{g kg}^{-1}$ at S4, in ‘Royal Gala’ and ‘Opal®’, respectively. After peaking at S4, IAA content in ‘Opal®’ apples declined to $0.5 \mu\text{g kg}^{-1}$ at S6 (Fig. 2A). The expression pattern of *MdARF5* was consistent in both cultivars, remaining below 0.1 MNE from S1 to S3, then significantly increasing to 0.3 MNE at S4. In ‘Opal®’ apples, *MdARF5* expression continued to rise, peaking at 0.5 MNE during both S5 and S6 (Figure S1A).

Conversely, ACC levels remained stable around 5 nmol kg^{-1} for most of the sampling points, but briefly rose to 7 nmol kg^{-1} at S4 in ‘Opal®’ apples and to 15 nmol kg^{-1} at S3 in ‘Royal Gala’ apples (Fig. 2B). ACO activity stayed below $0.02 \text{ nmol kg}^{-1} \text{ h}^{-1}$ until a significant increase to $0.07 \text{ nmol kg}^{-1} \text{ h}^{-1}$ was detected at S4 in ‘Royal Gala’ apples and to $0.11 \text{ nmol kg}^{-1} \text{ h}^{-1}$ at S5 and $0.21 \text{ nmol kg}^{-1} \text{ h}^{-1}$ at S6 in ‘Opal®’ apples (Fig. 2C). In parallel with changes in ACO activity, *MdACO1* gene expression rose from 0.15 MNE in the initial developmental stages to above 80 MNE at S5 and S6 in ‘Opal®’ apples and S4 in ‘Royal Gala’ apples (Figure S1C). However, differences in *MdACS3* were observed between both cultivars in the later developmental stages. Whilst *MdACS3* expression only rose to 0.90 MNE at S4 in ‘Royal Gala’ apples, expression levels were significantly higher in ‘Opal®’, reaching 1.85 MNE at S5 and 2.41 MNE at S6 (Figure S1B).

An increasing trend was also observed in the expression of *MdERF1* and *MdERF2*. The expression of *MdERF1* evolved similarly in ‘Opal®’ and ‘Royal Gala’, rising from below 5 MNE at S2 to 17 MNE at S4. The expression of *MdERF1* in ‘Opal®’ apples remained at the maximum in S5 and then decreased to 12 MNE at S6 (Figure S2E). In contrast, the increase in *MdERF2* expression occurred earlier in ‘Royal Gala’ than in ‘Opal®’. In ‘Royal Gala’ apples, *MdERF2* expression began increasing at S3, reaching a value of 10 MNE, then rose to 23 MNE at S4, whilst in ‘Opal®’ apples, it increased to 14 MNE at S5 and reached a maximum of 25 MNE at S6 (Figure S2F).

The most significant differences between ‘Opal®’ and ‘Royal Gala’ apples were observed in the expression of *MdETR1*. Whilst the expression of *MdETR1* in ‘Royal Gala’ and ‘Granny Smith’ apples followed the same trend and remained below 0.07 MNE, its expression in ‘Opal®’ apples increased to 0.13 MNE at S4 and remained at that level until harvest (Figure S2D).

Phenolic Compounds and Anthocyanins Evolution

The levels of chlorogenic acid, flavonol glycosides, dihydrochalcones, and flavanols presented a declining trend throughout fruit development in the three studied cultivars (Fig. 3). The most noticeable differences amongst cultivars were observed in the evolution of flavonol glycosides and

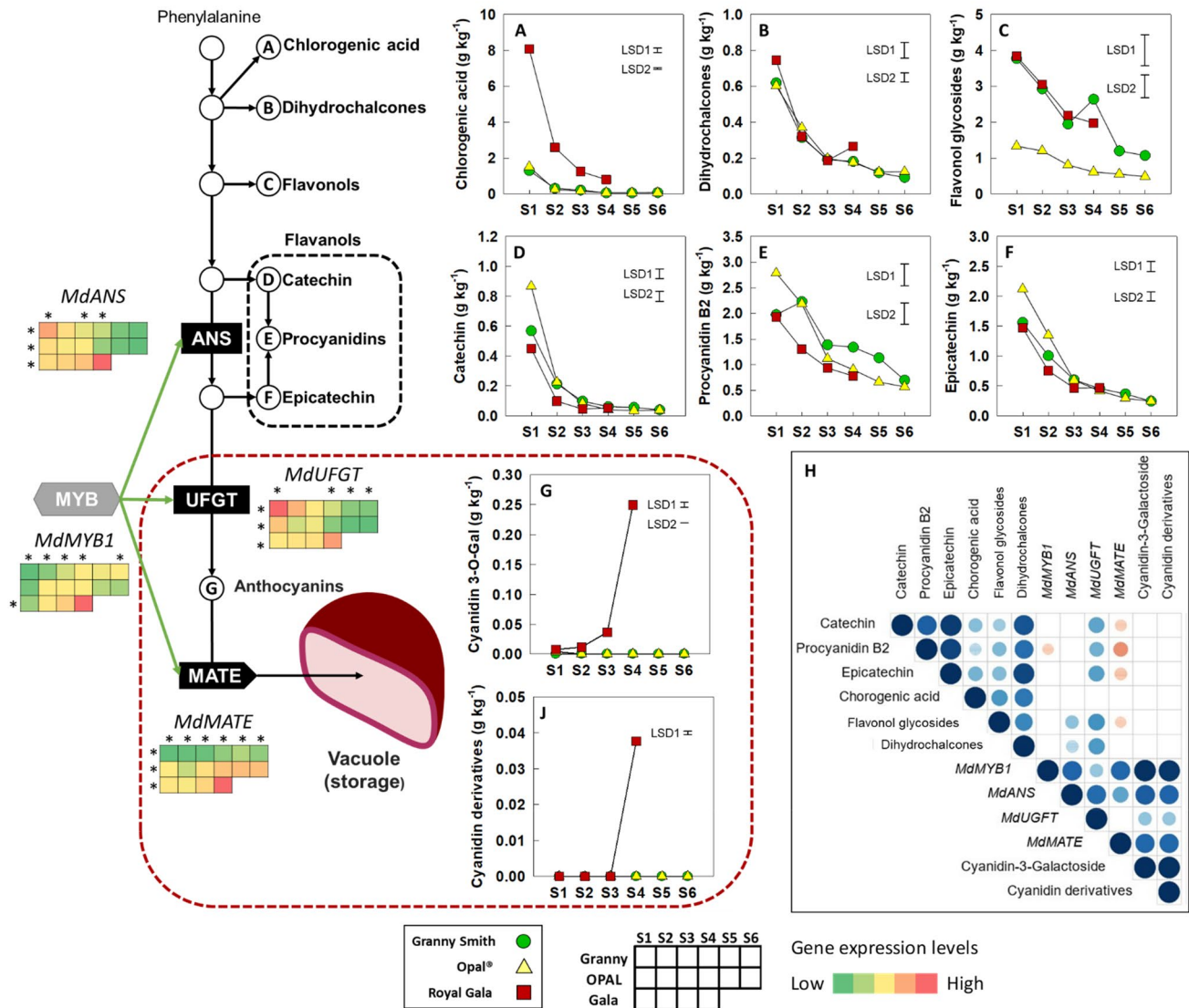


Fig. 3 Evolution of chlorogenic acid (A), dihydrochalcones (B), flavonol glycosides (C), catechin (D), procyanidin B2 (E), epicatechin (F), cyanidin-3-galactoside (G), cyanidin derivatives (J), and correlations amongst the parameters related with phenolic compounds metabolism (H) during the development and ripening of ‘Granny Smith’ (●), ‘Opal[®]’ (△) and ‘Royal Gala’ (■) apples. Green lines represent positive regulation. Each point represents the mean of four biological replicates (10 apples per replicate). Error bars represent the LSD values ($p=0.05$) for the interaction cultivar \times sampling point for all cultivars from S1 to S4 (LSD1) and for the interaction culti-

var \times sampling point for ‘Opal[®]’ and ‘Granny Smith’ from S1 to S6 (LSD2). The corresponding transcript levels of *MdANS*, *MdUFGT*, *MdMATE* and *MdMYB1* are represented as heatmaps. Significant differences ($p \leq 0.05$) amongst cultivars at the same sampling point are denoted by asterisks at the top of the heatmaps, whilst differences ($p \leq 0.05$) amongst sampling points at each specific cultivar are indicated by asterisks at the left of the heatmap. Green lines represent hypothetical positive regulation. The size of the circle for each correlation and the colour depicts the significance and the correlation coefficient, respectively. Positive correlation coefficients are displayed in blue and negative correlation coefficients in red

chlorogenic acid. Flavonol glycosides levels in ‘Opal[®]’ apples were less than half of those observed in ‘Granny Smith’ and ‘Royal Gala’ throughout the maturation process and presented a subtle decrease from 1.3 g kg⁻¹ at S1 to 0.5 kg⁻¹ at S4 and onwards (Fig. 3C). ‘Royal Gala’ presented the highest chlorogenic acid levels, which

decreased from 8.1 g kg⁻¹ at S1 to 0.8 g kg⁻¹ at S4. The remaining cultivars had significantly lower levels of chlorogenic acid, plummeting from 1.5 g kg⁻¹ at S1 to below 0.1 g kg⁻¹ at the S4 stage and beyond (Fig. 3A). Changes in procyanidin B2, catechin and epicatechin were similar

amongst cultivars and steadily declined as the fruit developed and ripened on-tree (Figs. 3D, E and F).

As expected, ‘Royal Gala’ was the only cultivar to exhibit an increase in anthocyanin concentration during development. A significant rise in cyanidin-3-O-galactoside levels was observed, beginning from S1 (0.01 g kg⁻¹) to S3 (0.04 g kg⁻¹), followed by a notable increase to 0.25 g kg⁻¹ at S4 (Fig. 3G). Other cyanidin derivatives were only detectable at the S4, achieving a concentration of 0.04 g kg⁻¹ (Fig. 3J). On the other hand, cyanidin-3-O-galactoside was only detected in ‘Opal[®]’ at S1, presenting a concentration of 0.01 g kg⁻¹, whilst ‘Granny Smith’ did not show detectable levels of anthocyanins at any stage of development or ripening (Fig. 3G).

Carotenoids and ABA Metabolism

All studied cultivars exhibited a general decline in total and individual carotenoid peel content throughout their development (Figs. 4 and S3A). Interestingly, ‘Granny Smith’ consistently exhibited the highest carotenoid concentration at each sampling point and its carotenoid levels underwent a more subtle drop if compared to ‘Opal[®]’ and ‘Royal Gala’, both of which revealed similar downward trends in their lutein, carotene, and neoxanthin levels. However, a noticeable difference was found in the levels of xanthophyll esters amongst these cultivars, with ‘Opal[®]’ reaching the highest levels at S5 and S6, with values of 3.0 mg kg⁻¹ and 4.5 mg kg⁻¹, respectively (Fig. 4C). On the other hand, the peel of ‘Royal Gala’ only had xanthophyll esters at S4 (0.5 mg kg⁻¹), whereas ‘Granny Smith’ did not show any detectable levels of these compounds (Fig. 4C).

Concerning ABA and their catabolites, ‘Granny Smith’ maintained stable basal levels whereas both ‘Opal[®]’ and ‘Royal Gala’ followed similar dynamic patterns (Figs. 4G and S4). ‘Opal[®]’ and ‘Royal Gala’ cultivars showed a concentration of ABA around 30 µg kg⁻¹ at S1, descended below 20 µg kg⁻¹ during S2 and S3 and then returned above 25 µg kg⁻¹ at S4 (Fig. 4G). Specifically, ‘Opal[®]’ preserved those elevated levels until stage S6. In general, the evolution of ABA catabolites (*viz.*, PA, neo-PA, DPA and 7-OH-ABA) followed a similar pattern as ABA (Figures S4A, S4B, S4D and S4E). However, ABA-GE substantially diverged from this pattern; in the peel of ‘Granny Smith’ and ‘Royal Gala’ ABA-GE concentrations remained consistently below 200 µg kg⁻¹, whereas in ‘Opal[®]’, levels sharply rose from S4, reaching 770 µg kg⁻¹ at S6 (Figure S4C).

The expression of *MdGGPPS* and *MdPSY*, which encode for the entry enzymes to the carotenoid pathway geranylgeranyl pyrophosphate synthase and phytoene synthase, remained basal in ‘Granny Smith’, whilst in ‘Opal[®]’ and ‘Royal Gala’, a parallel increase was noted from stage S3 onwards, reaching maximum gene expression at S4 in

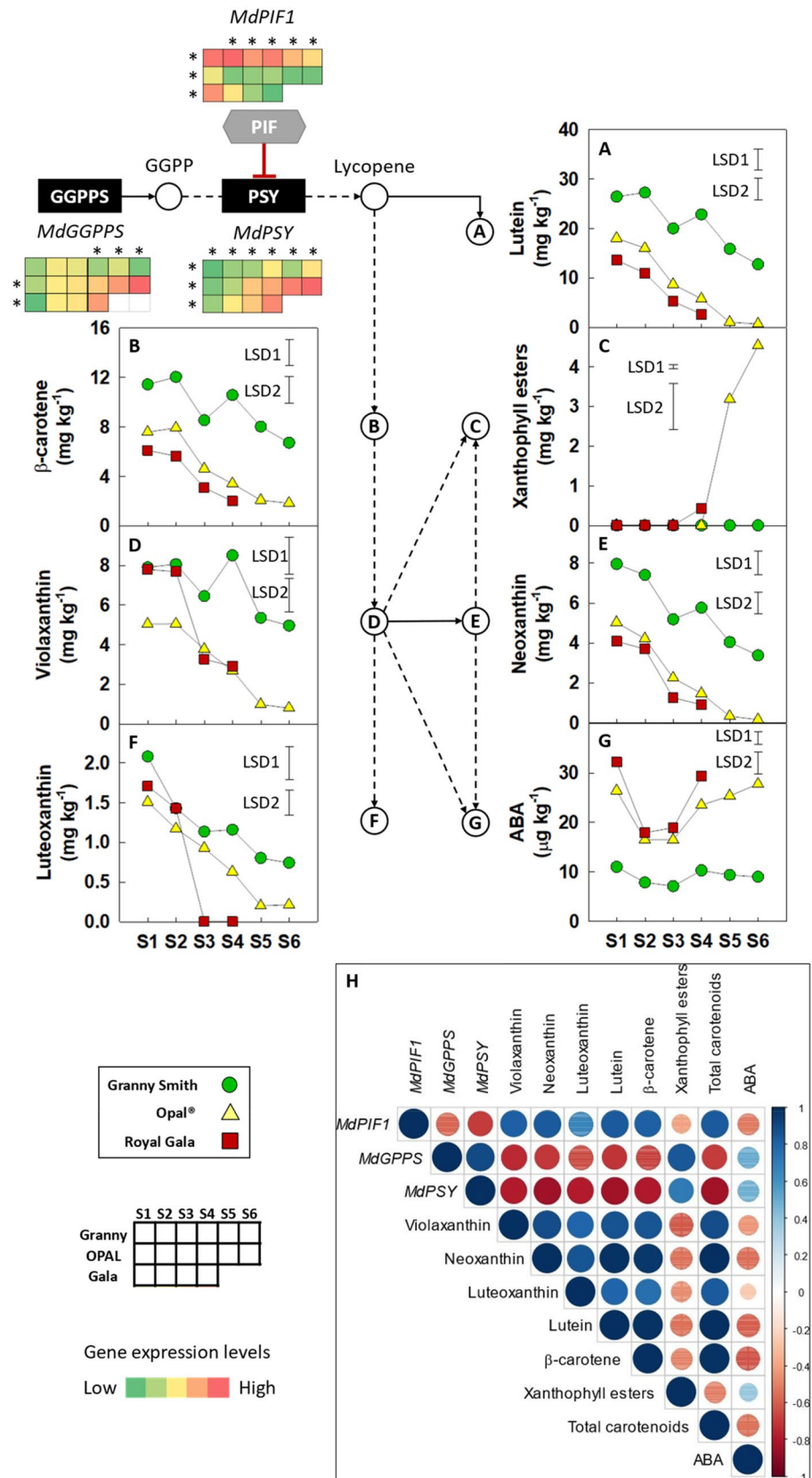
‘Royal Gala’ and at S6 in ‘Opal[®]’ (Figures S3C and S3D). In contrast, the transcription factor *MdPIF1* experienced a decrease in its expression as development progressed, although at varying rates across the cultivars (Figure S3B). In ‘Granny Smith’, *MdPIF1* expression remained above 0.20 MNE from stage S1 to S4, before descending to 0.13 MNE at stage S5 and finally 0.11 MNE at stage S6. The most profound decline was noted in ‘Royal Gala’, where its expression dropped from 0.19 MNE at S1 to a mere 0.02 MNE at S4. For ‘Opal[®]’, the expression decreased from 0.07 MNE at S1 to consistently below 0.05 MNE from S2 onwards.

Cytokinins and Chlorophyll Metabolism

Active cytokinin levels did not differ amongst cultivars, with all of them showing a decrease from 0.10 µg kg⁻¹ at S1 and S2 to less than 0.06 µg kg⁻¹ at S4 and subsequent stages. (Fig. 5A). A decreasing trend was also observed in the chlorophyll *a* levels in all studied cultivars throughout development (Fig. 5B). The peel of ‘Granny Smith’ exhibited the highest chlorophyll levels at all stages, presenting a slower reduction in chlorophyll content if compared to the other cultivars; with a decrease from 44.9 mg kg⁻¹ at S1 to 22.6 mg kg⁻¹ at S6. ‘Opal[®]’ demonstrated a significant decline, dropping from 34.1 mg kg⁻¹ at S1 to 1.4 mg kg⁻¹ at S6. ‘Royal Gala’ initially had the lowest concentration, around 22 mg kg⁻¹ at S1 and S2, before aligning with the content observed in the peel of ‘Opal[®]’ apples. Analogous patterns were detected for chlorophyll *b* evolution (Fig. 5C). Pheophytin *a* concentration peaked at S1 for all cultivars. Amongst them, ‘Granny Smith’ maintained the highest levels throughout development, beginning with 1.8 mg kg⁻¹ at S1, immediately decreasing to 0.5 mg kg⁻¹ at S2, and stabilizing at a steady 0.2 mg kg⁻¹ from S3 to S6. Pheophytin *a* levels in ‘Opal[®]’ and ‘Royal Gala’ were 0.8 mg kg⁻¹ and 0.3 mg kg⁻¹, respectively, at S1 but fell to undetectable levels in their later developmental stages (Fig. 5D).

The expression levels of the *GOLDEN2-LIKE* transcription factor, *MdGLK1*, involved in the regulation of chloroplast biogenesis, were the highest in ‘Granny Smith’ and the lowest in ‘Royal Gala’. In ‘Granny Smith’, *MdGLK1* expression remained around 1.0 from S1 to S3, peaked at 1.23 MNE at S4, and fell to 0.76 MNE at S5 and S6 (Figure S5A). In ‘OPAL[®]’, it remained stable at approximately 0.70 MNE from S1 to S4, then declined to 0.20 MNE at S5 and S6. On the other hand, ‘Royal Gala’ showed a stable decrease in *MdGLK1* transcription, shifting from 0.56 MNE at S1 to 0.09 MNE at S6. Regarding the genes involved in chlorophyll catabolism, transcription levels of *MdNYC1* stayed steady and under 0.25 MNE throughout ‘Granny Smith’

Fig. 4 Evolution of lutein (A), β -carotene (B), xanthophyll esters (C), violaxanthin (D), neoxanthin (E), luteoxanthin (F), ABA (G) and correlations amongst the parameters related with carotenoids metabolism (H) during the development and ripening of ‘Granny Smith’ (●), ‘Opal[®]’ (▲) and ‘Royal Gala’ (■) apples. Each point represents the mean of four biological replicates (10 apples per replicate). Error bars represent the LSD values ($p=0.05$) for the interaction cultivar \times sampling point for all cultivars from S1 to S4 (LSD1) and for the interaction cultivar \times sampling point for ‘Opal[®]’ and ‘Granny Smith’ from S1 to S6 (LSD2). The corresponding transcript levels of *MdPIF1*, *MdGGPPS* and *MdPSY* are represented as heatmaps. Significant differences ($p \leq 0.05$) amongst cultivars at the same sampling point are denoted by asterisks at the top of the heatmaps, whilst differences ($p \leq 0.05$) amongst sampling points at each specific cultivar are indicated by asterisks at the left of the heatmap. Red lines represent hypothetical negative regulation. The size of the circle for each correlation and the colour depicts the significance and the correlation coefficient, respectively. Positive correlation coefficients are displayed in blue and negative correlation coefficients in red



development (Fig. 5B) whereas for ‘Opal[®]’ and ‘Royal Gala’, *MdNYCI* expression followed a similar rising trend from around 0.30 MNE at S2 to 0.50 MNE at S4. The transcription of *MdPPH* displayed a regular upward trend in all three cultivars, peaking at 0.20 MNE at S4 (Figure S5C). Thereafter, both ‘Opal[®]’ and ‘Granny Smith’ had a decrease in their transcription levels, settling around 0.10 MNE at S5 and S6.

Discussion

Colour Changes may be Triggered by IAA-Ethylene Crosstalk

One of the most noticeable changes during apple development and ripening are the changes on peel colour (Ranganath 2022). Whilst it is widely known that, in apples, such colour changes are driven by the accumulation of specific pigments, not only pigment accumulation but more importantly the loss of chlorophyll seems responsible for such colour changes during the last stages of development and ripening in yellow peel apples (Fernández-Cancelo et al. 2022a). In these sense, the ability to change colour of ‘Opal[®]’ and ‘Royal Gala’ at different fruit developmental stages seemed to be mainly caused by a substantial chlorophyll loss, as demonstrated by the sharp decrease in I_{AD} (Fig. 1C) (Peifer et al. 2018). As a result, the carotenoids/chlorophylls and anthocyanins/chlorophylls ratios increased, and colour changes were noticeable at the later developmental stages of ‘Opal[®]’ and ‘Royal Gala’ apples (Figs. 1D and E). In contrast, the invariable I_{AD} values observed in ‘Granny Smith’ partially explain the lack of colour changes during its development (Fig. 1C), which can be attributed to the masking effect of chlorophyll on the contribution of other pigments to fruit colour (i.e. carotenoids) (Fernández-Cancelo et al. 2022a).

In apples, as well as in other climacteric fruit, the colour changes caused by chlorophyll loss and in some cases to the accumulation of anthocyanins and carotenoids during ripening are commonly linked to ethylene (Gao et al. 2020). This said, ethylene metabolism of apple peel during development is less studied than in pulp tissues (Whale and Singh 2007) and little or no information is currently available regarding the hormonal interplay in this specific tissue of apple fruit. Previous studies have shown that ethylene precursors, the activity of enzymes mediating the last steps of ethylene biosynthesis or the expression of genes involved in ethylene signalling and biosynthesis, strongly differ when comparing different apple tissues (Lara and Vendrell 2003; Rudell et al. 2000). When comparing different varieties (Fig. 2), our data showed that differences amongst cultivars regarding ethylene biosynthesis and signalling were mainly noticeable from S3 onwards

and generally agreed with previous studies on apple pulp tissue (Fernández-Cancelo et al. 2023). In these lines, and despite differences in absolute levels amongst apple tissues, it seems that the temporal changes in ethylene biosynthetic genes expression were quite consistent during apple peel or pulp development, although the expression pattern of *MdERFs* were tissue specific (Figure S1). Whereas no correlation was found amongst *MdERF1*, *MdERF2* and ethylene metabolism in pulp (Fernández-Cancelo et al., 2023), the expression of *MdERF1* and particularly *MdERF2* positively correlated with ethylene metabolism in the peel (Figure S6), likely due to their role in upregulating the expression of *MdACS3* in conjunction with *MdARF5* (Wang et al. 2007). In contrast, the limited transcription of *MdERF3* and minor variances in the expression patterns across cultivars (Figure S1G) probably discards its involvement in modulating ethylene metabolism during development and on-tree ripening.

Overall, our results further confirm that differences in colour changes amongst and within apple cultivars during development were associated to differences in the expression levels of ethylene biosynthetic enzymes and ACO activity, which, in turn, appeared to be positively regulated by IAA (Fig. 2). The high correlation amongst the transcription of genes involved in ethylene biosynthesis, *MdACS3* and *MdACO1* and the expression of *MdARF5* (Figs. 2 and S6) pointed out an active involvement of IAA in the activation of ethylene metabolism in the apple peel through the transcription factor *MdARF5*. These findings are in agreement with previous studies made in apple pulp (Fernandez-Cancelo et al. 2023; Busatto et al. 2021; Yue et al. 2020) and further reinforce the crosstalk between IAA and ethylene in regulating ripening-related changes of apples. In this context, the maintenance of IAA at basal levels and the low expression of *MdARF5* in ‘Granny Smith’ apples would be partly responsible for the above-mentioned low expression of *MdACS3* and *MdACO1*, as well as its minimal ACO activity in the peel of this apple cultivar (Fig. 2). Contrarily, the peel of ‘Royal Gala’ and ‘Opal[®]’ apples underwent a significant degreening process through development and on-tree ripening in parallel to the activation of ethylene metabolism (Figs. 1 and 2), which was possibly triggered by IAA as suggested not only by the positive correlation amongst IAA, *MdARF5* and ethylene metabolism observed in our study but also with the results from studies employing exogenous auxins treatments in apple (Yue et al. 2020).

Anthocyanins Accumulation is Regulated by MYB1 in an Ethylene-Dependent Manner

Chlorophylls, carotenoids and anthocyanins contribute to the green, yellow and red colours of apple peel, respectively. In yellow apple cultivars such as ‘Golden’ which present

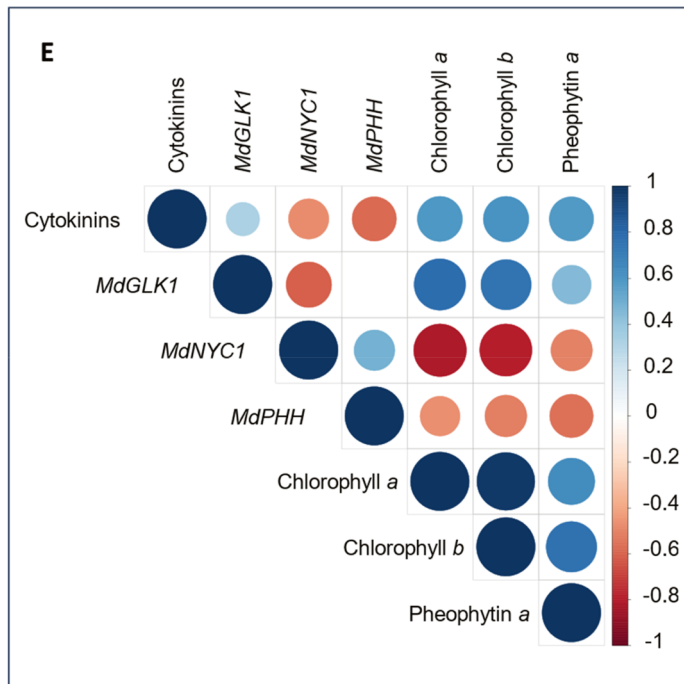
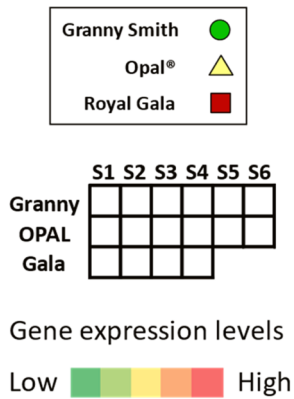
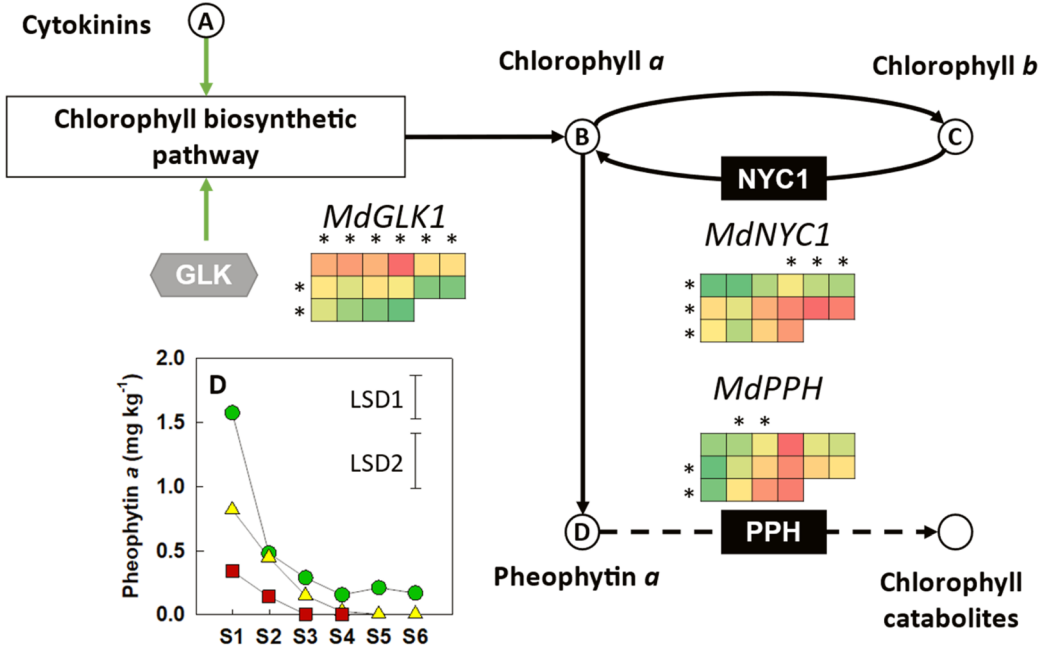
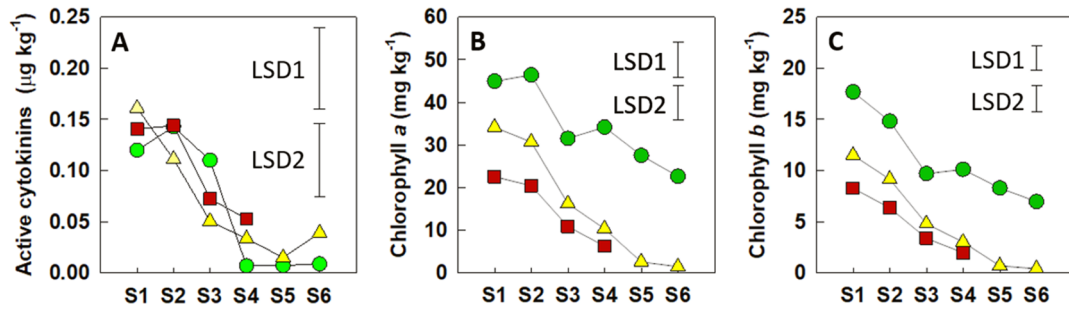


Fig. 5 Evolution of total cytokinins (A), chlorophyll *a* (B), chlorophyll *b* (C), pheophytin *a* (D) and correlations amongst the parameters related with chlorophyll metabolism (E) during the development and ripening of ‘Granny Smith’ (●), ‘Opal[®]’ (△) and ‘Royal Gala’ (■) apples. Each point represents the mean of four biological replicates (10 apples per replicate). Error bars represent the LSD values ($p=0.05$) for the interaction cultivar × sampling point for all cultivars from S1 to S4 (LSD1) and for the interaction cultivar × sampling point for ‘Opal[®]’ and ‘Granny Smith’ from S1 to S6 (LSD2). The corresponding transcript levels of *MdGLK1*, *MdNYC1* and *MdPPH* are represented as heatmaps. Significant differences ($p \leq 0.05$) amongst cultivars at the same sampling point are denoted by asterisks at the top of the heatmaps, whilst differences ($p \leq 0.05$) amongst sampling points at each specific cultivar are indicated by asterisks at the left of the heatmap. Green lines represent hypothetical positive regulation. The size of the circle for each correlation and the colour depicts the significance and the correlation coefficient, respectively. Positive correlation coefficients are displayed in blue and negative correlation coefficients in red

high carotenoids content during all developmental stages, the mere loss of chlorophyll during ripening is enough to trigger colour changes independently from the evolution of carotenoids levels (Fernández-Cancelo 2022a). However, in red-peel cultivars like ‘Royal Gala’, the loss of chlorophyll may not be sufficient to promote the appearance of red colour in this cultivar due to low levels of anthocyanins during most of the fruit development (S1 to S3) (Figs. 3G and J). Accordingly, the characteristic red colour of the ‘Royal Gala’ apple cultivar surged not exclusively due to a reduction in chlorophylls, but also through an increase in anthocyanin levels during fruit development (Figs. 3G and J) in a process that paralleled the decline of the rest of phenolic compounds (Fig. 3). The reduction of phenolic compounds was also observed in cultivars that did not accumulate anthocyanins, suggesting that substrate availability was not the limiting factor in anthocyanin biosynthesis for ‘Opal[®]’ and/or ‘Granny Smith’ apples.

Nevertheless, our data suggest that the accumulation of anthocyanins in ‘Royal Gala’ was primarily influenced by the transcription factor *MdMYB1*, a well-known positive regulator of anthocyanins biosynthetic genes, which was exclusively expressed in this cultivar (Figure S2D) (Wang et al. 2020a, b). In apples, *MdMYBA*, *MdMYB1*, and *MdMYB10* are alleles of a single locus in different genotypes mainly differing in a repeated sequence of the promoter region (Hu et al. 2016). *MdMYB10* is highly expressed in the apple pulp and foliage whereas *MdMYB1* and *MdMYBA* alleles are expressed only in apple peels (Espley et al. 2007; Lin-Wang et al. 2010). Our results showed that *MdMYB1* presented a positive correlation with anthocyanin biosynthetic genes (*MdANS* and *MdUFGT*) and, especially, with *MdMATE*, a gene associated with anthocyanin vacuolar transport (Hu et al. 2016) (Figure S6). Interestingly, both anthocyanins levels and *MdMYB1* expression followed the

same evolution as ACO activity in ‘Royal Gala’, suggesting a potential dependency of anthocyanins accumulation on ethylene production, and hence in agreement with other studies made in red apple cultivars (Wang et al. 2022). As pointed out by An et al. (2018), it is then feasible that the transcription factor *MdMYB1* plays a key role in the interplay between ethylene and anthocyanins metabolism, in coordination with other *MdERFs*. Indeed, some studies have shown that *MdERF3* (An et al. 2018) or *MdERF1* (Zhang et al. 2018) may play a key role in the ethylene-dependent regulation of red colour development of apples. Accordingly, our data further reinforce that *MdMYB1* may play a key role in the interplay between ethylene and anthocyanins metabolism of apple fruit likely via *MdERF1* and not *MdERF3*, since the expression of the former followed the same accumulation pattern than ACO, *MdMYB1* and anthocyanins content (Figures S1E, 2C, S2D and 3G).

Carotenoids Content is Regulated at Catabolic Level

Unlike anthocyanins, carotenoids level in the apple peel tended to decrease during fruit development in the three analysed cultivars, with the rate of carotenoid loss being cultivar dependent (Fig. 4). It is commonly accepted that higher pulp and peel carotenoid content is attributable to elevated activity of PSY. This enzyme catalyses the entrance in the carotenoids pathway to produce phytoene and is considered the limiting step in the carotenoid biosynthesis (Ampomah-Dwamena et al. 2022). However, our results showed a negative correlation between *MdPSY* and carotenoids, in agreement with previous studies made during development of ‘Golden Reinders’ apples (Fernández-Cancelo et al. 2022a). Our data also revealed a negative correlation between *MdPIF1* and *MdPSY* (Figs. 4H, S3B, S3D), indicating that PIF transcription factors may participate in the inhibition of *PSY* expression in apple, as already described for tomato and grape (Llorente et al. 2016; Zhuge et al. 2023). Although the regulatory role of *MdPIF1* seems to be cultivar dependent, its expression was not correlated with the evolution of any of the studied hormones, ethylene biosynthetic genes expression and ACO activity (Figure S6). Conversely, the expression of the entry genes into the carotenoid pathway (*MdGGPPS* and *MdPSY*) showed strong and positive correlation with *MdARF5*, ethylene biosynthetic genes (*MdASC3* and *MdACO1*), ACO activity and *MdERF2* (Figure S6). Despite correlation does not imply causation, this positive correlation may indicate that carotenogenic metabolism was triggered in response to an increase in ethylene biosynthetic metabolism in the last developmental stages of ‘Opal[®]’ and ‘Royal Gala’ and hence in agreement to that reported in apricot (Marty et al. 2005) and tomato (Lee et al. 2012).

Furthermore, the negative correlation amongst *MdGGPPS* and *MdPSY* with carotenes and xanthophylls levels

indicates that carotenoids content in apple peel may be regulated at the catabolic level (Figs. 4, S4 and S6). Indeed, the observed low ABA production and absence of xanthophyll ester biosynthesis in ‘Granny Smith’ might suggest an inhibition of carotenoid catabolism in this cultivar (Fig. 4C and G). In this sense, the reduced carotenoid catabolism in ‘Granny Smith’ could account, in turn, for its higher carotenoid content, regardless of its reduced *MdGGPPS* and *MdPSY* expression (Figures S3C and 3D). In contrast, the significant decrease in carotenoids levels in ‘Opal[®]’ and ‘Royal Gala’, especially in the final developmental stages, was likely the result of their usage as substrates for ABA and xanthophyll esters biosynthesis (Figs. 4 and S4).

The concomitant increase in ABA levels and *MdARF5* expression, alongside the activation of ethylene metabolism in ‘Opal[®]’ and ‘Royal Gala’ cultivars (Figs. 4G and S1), implies a possible ethylene-regulated mechanism for ABA biosynthesis, where specific genes or enzymes, such as NCED, could be activated as previously described in peach fruit (Wang et al. 2019). This regulatory mechanism could explain not only the results described herein but also the simultaneous increase in ethylene and ABA levels observed in apples during development and on-tree ripening (Fernández-Cancelo et al. 2023) as well as during postharvest ripening (Fernández-Cancelo et al. 2022b).

Nevertheless, the rise in ABA levels for both ‘Opal[®]’ and ‘Royal Gala’ did not proportionally correspond to the observed ACO activity changes (Figs. 2C and 4G). This discrepancy may arise due to variations in ABA catabolism across cultivars (Figure S4), which may be also regulated to some extent by ethylene (Figure S6) as pointed out for pepper (Hou et al. 2018). In particular, ‘Opal[®]’ exhibited a slower increase in ABA but a higher accumulation of ABA derivatives if compared to ‘Royal Gala’, which would further support an ethylene-dependent activation of ABA catabolic pathways (Figs. 4G and S4). Simultaneously, xanthophyll esters levels, considered indicators of ripening (Hornero-Méndez and Mínguez-Mosquera 2000), also showed a positive correlation with ethylene metabolism, suggesting a potential ethylene-mediated regulation of carotenoid esterification (Figure S6). However, studies in other apple cultivars showed that carotenoid esterification occurs independently of ethylene (Knee 1988), underlining the need for further research into the role of ethylene in activating xanthophylls esterification as well as ABA biosynthesis and catabolism.

Chlorophylls Levels may be Regulated by *MdGLK1*

Chlorophyll levels also decreased during apple development, although the rate and intensity of this decline was again cultivar dependent (Fig. 5B and C). ‘Granny Smith’ cultivar showed the most abundant chlorophyll levels at all sampling points, whilst ‘Opal[®]’ and ‘Royal Gala’ presented

lesser amounts. Intriguingly, the descending biologically active cytokinins content did not account for the observed discrepancies in chlorophyll content amongst the different cultivars, challenging the typical association between cytokinins and chlorophyll biosynthesis seen in other species (Cortleven and Schmölling 2015; Matsuo et al. 2012; Pilkington et al. 2013) (Fig. 5A). In this context, the role of *MdGLK1*, a transcription factor involved in chloroplast biogenesis, emerges as particularly significant in the regulation of chlorophyll levels in apple (An 2019; Chen et al. 2016) (Figure S5A). Our results showed that the expression of *MdGLK1* positively correlated with photosynthetic pigments levels (Fig. 5E). In several studies, phytohormones including auxin and brassinosteroids have been implicated in tomato fruit chloroplast development and positively correlated with increased *SIGLK* expression (Nadakuduti et al. 2014; Sagar et al. 2013). In our study, *MdGLK1* expression was negatively correlated to ethylene metabolism or auxin levels (Figure S6). Indeed, the sustained basal ethylene metabolism in ‘Granny Smith’ development upheld elevated *MdGLK1* expression and chlorophyll levels which masked the carotenoids contribution to peel colour and consequently inhibited colour changes in this specific cultivar. In turn, the rise in ethylene biosynthesis in the last stages of ‘Opal[®]’ and ‘Royal Gala’ development may downregulate *MdGLK1* and lead to a decrease in chlorophyll content, arising the colour changes associated with apple ripening in the last sampling points (Figs. 1, 2 and 5). However, catabolic pathways may also regulate chlorophylls content as suggested by the association between chlorophylls and *MdNYC1*, a gene which encodes the enzyme involved in chlorophyll *b* degradation. The expression of *MdNYC1* exhibited a positive correlation with ethylene metabolism, in agreement with prior research which demonstrated that ethylene promotes the expression of genes associated with chlorophyll catabolism (Figure S6) (Wei et al. 2021). On the other hand, the expression pattern of *MdPPH*, as well as the levels of pheophytin from S2 onwards, showed the same evolution in the three studied cultivars regardless of the hormonal dynamics (Figs. 5D and S5C). This behaviour suggests that the limiting step of chlorophyll catabolism may be located upstream in the pathway or that alternative routes may be used during apple chlorophyll degradation. Since chlorophyll loss is key for colour changes in apple, a deeper analysis of the environmental and developmental factors as well as the regulatory pathways involved in chlorophyll catabolism are necessary to understand in depth the colour evolution during apple fruit development and ripening.

Conclusion

The levels of pigment in apples seemed to be regulated differently depending on the developmental stage. Early during apple development, pigments appear to evolve independently of the hormones studied, suggesting that environmental and cultivar-specific factors could be the main regulators. However, as the fruit approached the final developmental stages, ethylene and its interplay with other hormones emerged as an important regulator of pigment levels in the apple peel. Specifically, colour changes in ‘Opal®’ and ‘Royal Gala’ cultivars seem to be linked to the activation of ethylene metabolism by IAA via *MdARF5*. In contrast, the persistence of a green colour in ‘Granny Smith’ apples can be attributed to the basal IAA and ethylene levels, hence not promoting chlorophyll losses, masking the contribution of carotenoids to the apple peel colour. Control of chlorophyll levels in apples appeared to occur both at the biosynthetic and catabolic level, mediated by *MdGLK1* and *MdNYC1*, respectively. Ethylene metabolism, IAA and ABA were negatively correlated with *MdGLK1* and positively correlated with *MdNYC1*, suggesting the potential influence of these hormones on determining chlorophyll content during the late developmental stages. The red colour of ‘Royal Gala’ apples occurred not only due to a decline in chlorophyll level but to an important accumulation of anthocyanins during fruit development, in a process regulated at the biosynthetic and storage levels by *MdMYB1*. In contrast, carotenoids levels tended to decrease, especially in ‘Opal®’ and ‘Royal Gala’ apples during the later stages of development, potentially due to their usage as substrates for ABA and xanthophyll esters biosynthesis, thereby, suggesting that carotenoid concentrations are primarily controlled at the catabolic level and that their contribution to the apple peel colour is somehow limited.

Whilst these findings provide a significant advance in our understanding of the complex hormonal mechanisms controlling apple colour changes, future research should explore the crosstalk between environmental and developmental factors on the regulation of pigments metabolism.

Supplementary Information The online version contains supplementary material available at <https://doi.org/10.1007/s00344-024-11270-6>.

Acknowledgements This work has been partially financially supported by the Spanish Agencia Estatal de Investigación (AEI) and European Regional Development Fund (ERDF) through the national project PID2020-117607RR-I00 (ENVIRONAPPLE). This work has been also supported by the 2021 SGR 01477 grant and CERCA Programme from the ‘Generalitat de Catalunya’. Thanks are also given to AEI and ERDF for the predoctoral fellowship awarded to PFC (BES-2017-080741). We are also grateful to Monika Jodkowska and Dr. Emma Collings, at Cranfield University, and Dr. Núria Vall-Illaura for their indispensable and outstanding technical support.

Author Contributions JGB and PFC: conceived and designed the experiments. PFC: carried out the experiments. MCA and PFC: were responsible for the quantification of hormones and phenylpropanoids. NT: assisted with the statistical analysis and data interpretation. JGB, NT, and MCA: were responsible for the project resources. PFC and JGB: drafted the manuscript and all other authors contributed to improving the definitive version of the manuscript.

Funding Spanish Agencia Estatal de Investigación (AEI) and European Regional Development Fund (ERDF), PID2020-117607RR-I00, Jordi Giné-Bordonaba; CERCA Programme from the ‘Generalitat de Catalunya’; Agencia Estatal de Investigación (AEI); and European Regional Development Fund (ERDF), BES-2017-080741, Pablo Fernández-Cancelo.

Data availability The underlying data for this research work can be found in can be found in CORD using the following link <https://doi.org/10.17862/cranfield.rd.25479649>.

Declarations

Conflict of interest The authors declare that they have no known competing financial interests or personal relationships that could have appeared to influence the work reported in this paper.

Open Access This article is licensed under a Creative Commons Attribution 4.0 International License, which permits use, sharing, adaptation, distribution and reproduction in any medium or format, as long as you give appropriate credit to the original author(s) and the source, provide a link to the Creative Commons licence, and indicate if changes were made. The images or other third party material in this article are included in the article’s Creative Commons licence, unless indicated otherwise in a credit line to the material. If material is not included in the article’s Creative Commons licence and your intended use is not permitted by statutory regulation or exceeds the permitted use, you will need to obtain permission directly from the copyright holder. To view a copy of this licence, visit <http://creativecommons.org/licenses/by/4.0/>.

References

- Alagoz Y, Dhami N, Mitchell C, Cazzonelli CI (2020) cis/trans Carotenoid Extraction, Purification, Detection, Quantification, and Profiling in Plant Tissues. In: Rodríguez-Concepción M, Welsch R (eds) Plant and Food Carotenoids, Methods in Molecular Biology. Springer, New York, pp 145–163
- Ampomah-Dwamena C, Driedonks N, Lewis D, Shumskaya M, Chen X, Wurtzel ET, Espley RV, Allan AC (2015) The Phytoene synthase gene family of apple (*Malus x domestica*) and its role in controlling fruit carotenoid content. BMC Plant Biol 15:185. <https://doi.org/10.1186/s12870-015-0573-7>
- Ampomah-Dwamena C, Tomes S, Thrimawithana AH, Elborough C, Bhargava N, Rebstock R, Sutherland P, Ireland H, Allan AC, Espley RV (2022) Overexpression of PSY1 increases fruit skin and flesh carotenoid content and reveals associated transcription factors in apple (*Malus x domestica*). Front Plant Sci 13:967143. <https://doi.org/10.3389/fpls.2022.967143>
- An X-H (2019) Functional identification of apple *MdGLK1* which regulates chlorophyll biosynthesis in arabiDOPSIS. J Plant Growth Regul 38(3):778–787
- An J-P, Wang X-F, Li Y-Y, Song L-Q, Zhao L-L, You C-X, Hao Y-J (2018) EIN3-LIKE1, MYB1, and ETHYLENE RESPONSE FACTOR3 act in a regulatory loop that synergistically modulates

- ethylene biosynthesis and anthocyanin accumulation. *Plant Physiol* 178:808–823. <https://doi.org/10.1104/pp.18.00068>
- Anastasiadi M, Mohareb F, Redfern SP, Berry M, Simmonds MSJ, Terry LA (2017) Biochemical profile of heritage and modern apple cultivars and application of machine learning methods to predict usage, age, and harvest season. *J Agric Food Chem* 65:5339–5356. <https://doi.org/10.1021/acs.jafc.7b00500>
- Busatto N, Tadiello A, Moretto M, Farneti B, Populin F, Vrhovsek U, Comisso M, Sartori E, Sonogo P, Biasioli F, Costa G, Guzzo F, Fontana P, Engelen K, Costa F (2021) Ethylene-auxin crosstalk regulates postharvest fruit ripening process in apple. *Fruit Res* 1:1–13. <https://doi.org/10.48130/FruRes-2021-0013>
- Cackett L, Luginbuehl LH, Schreier TB, Lopez-Juez E, Hibberd JM (2022) Chloroplast development in green plant tissues: the interplay between light, hormone, and transcriptional regulation. *New Phytol* 233:2000–2016. <https://doi.org/10.1111/nph.17839>
- Chaabouni S, Jones B, Delalande C, Wang H, Li Z, Mila I, Frasse P, Latché A, Pech J-C, Bouzayen M (2009) SI-IAA3, a tomato Aux/IAA at the crossroads of auxin and ethylene signalling involved in differential growth. *J Exp Bot* 60:1349–1362. <https://doi.org/10.1093/jxb/erp009>
- Chen M, Ji M, Wen B, Liu L, Li S, Chen X, Gao D, Li L (2016) GOLDEN 2-LIKE transcription factors of plants. *Front Plant Sci*. <https://doi.org/10.3389/fpls.2016.01509>
- Collings E, Landahl S, Jodkowska M, Nayakoti S, Chinn J, Rogers H, Terry LA, Alamar MC (2023) Understanding the mechanisms responsible for postharvest tip breakdown in asparagus: a biochemical approach. *Acta Horticult* 1376:233–240. <https://doi.org/10.17660/ActaHortic.2023.1376.32>
- Cortleven A, Schmülling T (2015) Regulation of chloroplast development and function by cytokinin. *EXBOTJ* 66:4999–5013. <https://doi.org/10.1093/jxb/erv132>
- Cruz AB, Bianchetti RE, Alves FRR, Purgatto E, Peres LEP, Rossi M, Freschi L (2018) Light, ethylene and auxin signaling interaction regulates carotenoid biosynthesis during tomato fruit ripening. *Front Plant Sci* 9:1370. <https://doi.org/10.3389/fpls.2018.01370>
- Dar JA, Wani AA, Ahmed M, Nazir R, Zargar SM, Javaid K (2019) Peel colour in apple (*Malus × domestica* Borkh.): an economic quality parameter in fruit market. *Sci Hortic* 244:50–60. <https://doi.org/10.1016/j.scienta.2018.09.029>
- De Pascual-Teresa S, Sanchez-Ballesta MT (2008) Anthocyanins: from plant to health. *Phytochem Rev* 7:281–299. <https://doi.org/10.1007/s1101-007-9074-0>
- Eggersdorfer M, Wyss A (2018) Carotenoids in human nutrition and health. *Arch Biochem Biophys* 652:18–26. <https://doi.org/10.1016/j.abb.2018.06.001>
- Espley RV, Hellens RP, Putterill J, Stevenson DE, Kuty-Amma S, Allan AC (2007) Red colouration in apple fruit is due to the activity of the MYB transcription factor, *MdMYB10*: A MYB transcription factor controlling apple fruit colour. *Plant J* 49:414–427. <https://doi.org/10.1111/j.1365-313X.2006.02964.x>
- Fernández-Cancelo P, Iglesias-Sánchez A, Torres-Montilla S, Ribas-Agustí A, Teixidó N, Rodríguez-Concepción M, Giné-Bordonaba J (2022a) Environmentally driven transcriptomic and metabolic changes leading to color differences in “Golden Reinders” apples. *Front Plant Sci* 13:913433. <https://doi.org/10.3389/fpls.2022.913433>
- Fernández-Cancelo P, Muñoz P, Echeverría G, Larrigaudière C, Teixidó N, Munné-Bosch S, Giné-Bordonaba J (2022b) Ethylene and abscisic acid play a key role in modulating apple ripening after harvest and after cold-storage. *Postharvest Biol Technol* 188:111902. <https://doi.org/10.1016/j.postharvbio.2022.111902>
- Fernández-Cancelo P, Echeverría G, Teixidó N, Alamar MC, Giné-Bordonaba J (2023) Cultivar differences in the hormonal crosstalk regulating apple fruit development and ripening: relationship with flavour components and postharvest susceptibility to *Penicillium expansum*. *Postharvest Biol Technol* 205:112532. <https://doi.org/10.1016/j.postharvbio.2023.112532>
- Gao J, Zhang Y, Li Z, Liu M (2020) Role of ethylene response factors (ERFs) in fruit ripening. *Food Qual Saf* 4(1):15–20
- García-Pastor ME, Falagán N, Giné-Bordonaba J, Wójcik DA, Terry LA, Alamar MC (2021) Cultivar and tissue-specific changes of abscisic acid, its catabolites and individual sugars during postharvest handling of flat peaches (*Prunus persica* cv. platycarpa). *Postharvest Biol Technol* 181:111688. <https://doi.org/10.1016/j.postharvbio.2021.111688>
- Gupta K, Wani SH, Razzaq A, Skalicky M, Samantara K, Gupta S, Pandita D, Goel S, Grewal S, Hejnak V, Shiv A, El-Sabroun AM, Elansary HO, Alaklabi A, Brestic M (2022) Abscisic acid: role in fruit development and ripening. *Front Plant Sci* 13:817500. <https://doi.org/10.3389/fpls.2022.817500>
- Hornero-Méndez D, Mínguez-Mosquera MI (2000) Xanthophyll esterification accompanying carotenoid overaccumulation in chromoplast of *Capsicum annuum* ripening fruits is a constitutive process and useful for ripeness index. *J Agric Food Chem* 48:1617–1622. <https://doi.org/10.1021/jf9912046>
- Hou B-Z, Li C-L, Han Y-Y, Shen Y-Y (2018) Characterization of the hot pepper (*Capsicum frutescens*) fruit ripening regulated by ethylene and ABA. *BMC Plant Biol* 18:162. <https://doi.org/10.1186/s12870-018-1377-3>
- Hu D-G, Sun C-H, Ma Q-J, You C-X, Cheng L, Hao Y-J (2016) MdMYB1 regulates anthocyanin and malate accumulation by directly facilitating their transport into vacuoles in apples. *Plant Physiol* 170:1315–1330. <https://doi.org/10.1104/pp.15.01333>
- Knee M (1972) Anthocyanin, Carotenoid, and chlorophyll changes in the peel of Cox’s orange pippin apples during ripening on and off the tree. *J Exp Bot* 23:184–196. <https://doi.org/10.1093/jxb/23.1.184>
- Knee M (1988) Carotenol esters in developing apple fruits. *Phytochemistry* 27:1005–1009. [https://doi.org/10.1016/0031-9422\(88\)80261-9](https://doi.org/10.1016/0031-9422(88)80261-9)
- Lara I, Vendrell M (2003) Cold-induced ethylene biosynthesis is differentially regulated in peel and pulp tissues of ‘Granny Smith’ apple fruit. *Postharvest Biol Technol* 29:109–119. [https://doi.org/10.1016/S0925-5214\(02\)00243-0](https://doi.org/10.1016/S0925-5214(02)00243-0)
- Lee JM, Joung J-G, McQuinn R, Chung M-Y, Fei Z, Tieman D, Klee H, Giovannoni J (2012) Combined transcriptome, genetic diversity and metabolite profiling in tomato fruit reveals that the ethylene response factor *S1ERF6* plays an important role in ripening and carotenoid accumulation: Ripening factor identified through systems analysis. *Plant J* 70:191–204. <https://doi.org/10.1111/j.1365-313X.2011.04863.x>
- Lindo-García V, Muñoz P, Larrigaudière C, Munné-Bosch S, Giné-Bordonaba J (2020) Interplay between hormones and assimilates during pear development and ripening and its relationship with the fruit postharvest behaviour. *Plant Sci* 291:110339. <https://doi.org/10.1016/j.plantsci.2019.110339>
- Lin-Wang K, Bolitho K, Grafton K, Kortstee A, Karunairatnam S, McGhie TK, Espley RV, Hellens RP, Allan AC (2010) An R2R3 MYB transcription factor associated with regulation of the anthocyanin biosynthetic pathway in Rosaceae. *BMC Plant Biol* 10:50. <https://doi.org/10.1186/1471-2229-10-50>
- Liu H, Liu Z, Wu Y, Zheng L, Zhang G (2021) Regulatory mechanisms of anthocyanin biosynthesis in apple and pear. *IJMS* 22:8441. <https://doi.org/10.3390/ijms22168441>
- Llorente B, D’Andrea L, Ruiz-Sola MA, Botterweg E, Pulido P, Andilla J, Loza-Alvarez P, Rodríguez-Concepción M (2016) Tomato fruit carotenoid biosynthesis is adjusted to actual ripening progression by a light-dependent mechanism. *Plant J* 85:107–119. <https://doi.org/10.1111/tpj.13094>

- Lucas M, Prat S (2014) PIFs get BR right: PHYTOCHROME INTERACTING FACTORS as integrators of light and hormonal signals. *New Phytol* 202:1126–1141. <https://doi.org/10.1111/nph.12725>
- Marty I, Bureau S, Sarkissian G, Gouble B, Audergon JM, Albagnac G (2005) Ethylene regulation of carotenoid accumulation and carotenogenic gene expression in colour-contrasted apricot varieties (*Prunus armeniaca*). *J Exp Bot* 56:1877–1886. <https://doi.org/10.1093/jxb/eri177>
- Matsuo S, Kikuchi K, Fukuda M, Honda I, Imanishi S (2012) Roles and regulation of cytokinins in tomato fruit development. *J Exp Bot* 63:5569–5579. <https://doi.org/10.1093/jxb/ers207>
- Mou W, Li D, Bu J, Jiang Y, Khan ZU, Luo Z, Mao L, Ying T (2016) Comprehensive analysis of ABA Effects on ethylene biosynthesis and signaling during tomato fruit ripening. *PLoS ONE* 11:e0154072. <https://doi.org/10.1371/journal.pone.0154072>
- Muller PY, Janovjak H, Miserez AR, Dobbie Z (2002) Short technical report processing of gene expression data generated by quantitative real-time RT-PCR. *Biotechniques* 32:1372–1379
- Nadakuduti SS, Holdsworth WL, Klein CL, Barry CS (2014) KNOX genes influence a gradient of fruit chloroplast development through regulation of GOLDEN2-LIKE expression in tomato. *Plant J* 78:1022–1033. <https://doi.org/10.1111/tpj.12529>
- Peifer L, Ottmad S, Kunz A, Damerow L, Blanke M (2018) Effect of non-chemical crop load regulation on apple fruit quality, assessed by the DA-meter. *Sci Hortic* 233:526–531. <https://doi.org/10.1016/j.scienta.2017.11.011>
- Pilkington SM, Montefiori M, Galer AL, Neil Emery RJ, Allan AC, Jameson PE (2013) Endogenous cytokinin in developing kiwifruit is implicated in maintaining fruit flesh chlorophyll levels. *Ann Bot* 112:57–68. <https://doi.org/10.1093/aob/mct093>
- Ranganath KG (2022) Pigments that colour our fruits: an overview. *Erwerbs-Obstbau*. <https://doi.org/10.1007/s10341-022-00698-3>
- Reay PF, Fletcher RH, Thomas VJ, (Gary), (1998) Chlorophylls, carotenoids and anthocyanin concentrations in the skin of ‘Gala’ apples during maturation and the influence of foliar applications of nitrogen and magnesium. *J Sci Food Agric* 76:63–71. [https://doi.org/10.1002/\(SICI\)1097-0010\(199801\)76:1%3c63::AID-JSFA908%3e3.0.CO;2-K](https://doi.org/10.1002/(SICI)1097-0010(199801)76:1%3c63::AID-JSFA908%3e3.0.CO;2-K)
- Rudell DR, Mattinson DS, Fellman JK, Mattheis JP (2000) The progression of ethylene production and respiration in the tissues of ripening ‘Fuji’ apple fruit. *HortSci* 35:1300–1303. <https://doi.org/10.21273/HORTSCI.35.7.1300>
- Sagar M, Chervin C, Mila I, Hao Y, Roustan J-P, Benichou M, Gibon Y, Biais B, Maury P, Latché A, Pech J-C, Bouzayen M, Zouine M (2013) SIARF4, an auxin response factor involved in the control of sugar metabolism during tomato fruit development. *Plant Physiol* 161:1362–1374. <https://doi.org/10.1104/pp.113.213843>
- Scalisi A, O’Connell MG, Islam MS, Goodwin I (2022) A Fruit Colour development index (CDI) to Support harvest time decisions in peach and nectarine orchards. *Horticulturae* 8:459. <https://doi.org/10.3390/horticulturae8050459>
- Tatsuki M, Nakajima N, Fujii H, Shimada T, Nakano M, Hayashi K, Hayama H, Yoshioka H, Nakamura Y (2013) Increased levels of IAA are required for system 2 ethylene synthesis causing fruit softening in peach (*Prunus persica L. Batsch*). *J Exp Bot* 64:1049–1059. <https://doi.org/10.1093/jxb/ers381>
- Wang A, Tan D, Takahashi A, Zhong Li T, Harada T (2007) *MdERFs*, two ethylene-response factors involved in apple fruit ripening. *J Exp Bot* 58:3743–3748. <https://doi.org/10.1093/jxb/erm224>
- Wang X, Zeng W, Ding Y, Wang Y, Niu L, Yao J-L, Pan L, Lu Z, Cui G, Li G, Wang Z (2019) *PpERF3* positively regulates ABA biosynthesis by activating *PpNCED2/3* transcription during fruit ripening in peach. *Hortic Res* 6:19. <https://doi.org/10.1038/s41438-018-0094-2>
- Wang Q, Liu H, Zhang M, Liu S, Hao Y, Zhang Y (2020a) *MdMYC2* and *MdERF3* positively co-regulate α -farnesene biosynthesis in apple. *Front Plant Sci* 11:512844. <https://doi.org/10.3389/fpls.2020.512844>
- Wang W, Celton J-M, Buck-Sorlin G, Balzergue S, Bucher E, Laurens F (2020b) Skin color in apple fruit (*Malus × domestica*): genetic and epigenetic insights. *Epigenomes* 4:13. <https://doi.org/10.3390/epigenomes4030013>
- Wang S, Li L-X, Fang Y, Li D, Mao Z, Zhu Z, Chen X-S, Feng S-Q (2022) *MdERF1B*–*MdMYC2* module integrates ethylene and jasmonic acid to regulate the biosynthesis of anthocyanin in apple. *Hortic Res*. <https://doi.org/10.1093/hr/uhac142>
- Wei Y, Jin J, Xu Y, Liu W, Yang G, Bu H, Li T, Wang A (2021) Ethylene-activated *MdPUB24* mediates ubiquitination of *MdBEL7* to promote chlorophyll degradation in apple fruit. *Plant J* 108:169–182. <https://doi.org/10.1111/tpj.15432>
- Whale SK, Singh Z (2007) Endogenous Ethylene and color development in the skin of ‘Pink Lady’ apple. *J Amer Soc Hort Sci* 132:20–28. <https://doi.org/10.21273/JASHS.132.1.20>
- Yue P, Lu Q, Liu Z, Lv T, Li X, Bu H, Liu W, Xu Y, Yuan H, Wang A (2020) Auxin-activated *MdARF5* induces the expression of ethylene biosynthetic genes to initiate apple fruit ripening. *New Phytol* 226:1781–1795. <https://doi.org/10.1111/nph.16500>
- Zhang B, Peng B, Zhang C, Song Z, Ma R (2017) Determination of fruit maturity and its prediction model based on the pericarp index of absorbance difference (I_{AD}) for peaches. *PLoS ONE* 12:e0177511. <https://doi.org/10.1371/journal.pone.0177511>
- Zhang J, Xu H, Wang N, Jiang S, Fang H, Zhang Z, Yang G, Wang Y, Su M, Xu L, Chen X (2018) The ethylene response factor *MdERF1B* regulates anthocyanin and proanthocyanidin biosynthesis in apple. *Plant Mol Biol* 98:205–218. <https://doi.org/10.1007/s11103-018-0770-5>
- Zhou X, Rao S, Wrightstone E, Sun T, Lui ACW, Welsch R, Li L (2022) Phytoene synthase: the key rate-limiting enzyme of carotenoid biosynthesis in plants. *Front Plant Sci* 13:884720. <https://doi.org/10.3389/fpls.2022.884720>
- Zhuge Y, Sheng H, Zhang M, Fang J, Lu S (2023) Grape phytochrome-interacting factor *VvPIF1* negatively regulates carotenoid biosynthesis by repressing *VvPSY* expression. *Plant Sci* 331:111693. <https://doi.org/10.1016/j.plantsci.2023.111693>

Publisher's Note Springer Nature remains neutral with regard to jurisdictional claims in published maps and institutional affiliations.